

## **Simulation-aided computed tomography (CT) for dimensional measurements**

Uwe Hilpert <sup>1</sup>, Markus Bartscher <sup>1</sup>, Michael Neugebauer <sup>1</sup>,  
Jürgen Goebbels <sup>2</sup>, Gerd Weidemann <sup>2</sup>, Carsten Bellon <sup>2</sup>

<sup>1</sup> Physikalisch-Technische Bundesanstalt

38116 Braunschweig, Germany; Phone: +49 531 592 5217, Fax +49 531 592 69 5217;  
uwe.hilpert@ptb.de, markus.bartscher@ptb.de, michael.neugebauer@ptb.de

<sup>2</sup> Bundesanstalt für Materialforschung und -prüfung, Division VIII.3 Radiological Methods  
12205 Berlin, Germany; Phone: +49 30 8104 4106, Fax +49 30 8104 1837;  
juergen.goebbels@bam.de, gerd.weidemann@bam.de, carsten.bellon@bam.de

### **Abstract**

Carrying out dimensional measurements by CT means assessing coordinates in space. CT must therefore be treated as a coordinate measuring technique similar to optical or tactile Coordinate Measuring Machines (CMMs). The well-established standards and guidelines for the acceptance- and verification-testing of CMMs require the use of calibrated reference standards to achieve measurement machine characteristics.

Hence, transferring these concepts from coordinate metrology to CT, a dedicated CT-specific reference standard was designed, manufactured and calibrated using a tactile CMM. For comparison purposes, a CAD model was created by reverse engineering using the calibration data. The calibrated model was fed into a virtual CT and the measurement process was simulated. The reference standard was measured by micro-CT.

By comparing the characteristics of the measurement output of CT and the output gained from simulation, the influences of measurement artefacts can be judged, for the first time, in analogy to existing guidelines of coordinate metrology.

**Keywords:** Computed Tomography, Industrial CT, X-ray, Simulation, Coordinate Metrology

## **1. Introduction**

Computed tomography (CT) using X-rays is a well-established imaging technology in medical diagnostics. The principle of tomographic reconstruction first applied with CT imaging in the early 70s of the last century has been used for further medical sensing techniques such as positron emission tomography (PET), single photon emission tomography (SPECT), and magnetic resonance tomography (MRT). Today, medical CT systems already feature the 5th generation [1].

The attractiveness of these technologies lies in the fact that they furnish, in their common performance and within a short period of time, precise quantitative information on the whole structure of a body without destroying it. This is what has made CT very interesting for testing, and inspecting manufactured workpieces like engine blocks, gear boxes or even injection nozzles. Hence, dedicated industrial CT systems have, since the middle of the 80s of the last century, been in use for nondestructive testing, and for some years also for dimensional measurements.

## **2. Simulation-aided Computed Tomography**

If CT is to be established as a new coordinate measuring technique, first of all the uncertainty of measurement has to be determined. However, ongoing studies on this matter are very time-consuming and cost-intensive and, in many cases, not practicable.

According to the GUM 'Guide to the Expression of Uncertainty in Measurement' [2], there are several possibilities of investigating the uncertainty of measurement. In one case, the uncertainty is calculated on the basis of a statistical analysis of repeated measurements of a calibrated workpiece. In another case, the additional aid of simulation is possible. The simulation approach is very attractive, if there is no closed budget of quantifiable influences available. In addition, it offers advantages in cases where the measurement tasks frequently change. As the measurement uncertainty is task dependent, it is, in practice, much easier to carry out 25 or more simulations with parameters which vary within reasonable limits, than, e.g. 25 real CT measurements. Furthermore, it is possible to acquire a set of optimal measurement parameters for a given object ab initio, even before the first measurement is performed. Another point is that simulation software can also be used to optimize the development process of CT systems, as it allows the manufacturer to design customer-specific CT-systems within a short time. From a more scientific, i.e. metrological, point of view, it is important to understand the measurement process itself. By simulating the CT process, it is possible to separate and quantify measurement influences that can lead to dimensional deviations. Thus, corrections may be deduced for the measurement once understanding the origin of the measurement deviations.

But in general, the question may be asked, whether the use of simulation brings about any disadvantage. The answer is yes, there are some restrictions when using simulation software. Mercifully, the list is short, although of fundamental importance:

Performing simulations requires the use of input data for the process. Also, the accuracy of the simulation process itself, especially the correctness of the model applied, must be evaluated.

In the following, a concept will be presented which is to show solutions to the problems through the application of existing guidelines from the field of coordinate metrology on the basis of a CT-adapted reference standard and procedures.

### ***2.1 Industrial CT system set-up***

CT systems consist of an X-ray source, a rotary table, an X-ray detector and a powerful data processing unit to compute, display and analyse the measurement results. Modern industrial CT systems differ from their medical counterparts in so far as the measurement object rotates on a rotary table. The measurement chain of industrial CT starts with the X-ray source, where X-rays are emitted by tubes of up to 450 kV acceleration voltage. Depending on whether a collimated fan beam in combination with a line (1D) detector, or a cone beam with an area (2D) detector is used, CT systems measure either 2D information (2D-CT) or 3D information (3D-CT) with one revolution of the part, respectively. To scan an object completely with 2D-CT, a coupled translation of source and detector is necessary as these systems measure the object successively in thin slices. In the case of 3D-CT, objects which fit entirely into the cone beam can be measured with just one revolution of the rotary table. A linear translation of source and detector is not necessary. This is why 3D-CT offers speed advantages compared to 2D-CT.

The contrast of CT is produced by X-ray absorption and is thus a function of the electron density of the object. After recording the X-ray projections, the object is numerically reconstructed. The 3D grey value data structure gained in this way represents the electron density distribution in the measured object. The primitive

elements of the digitized 3D data structure of the object are called voxels (an abbreviation of volumetric pixels).

Industrial CT systems can be classified into macro-CT systems for large [3] and micro-CT systems [4] for small measurement objects. By using X-ray tubes with small focal spots and by positioning the object close to the focus, a geometrical magnification is achieved by micro CT.

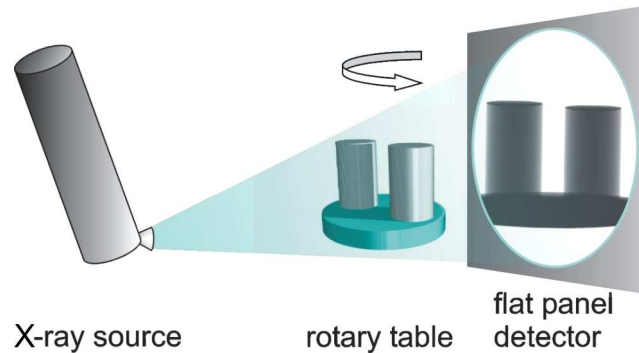


Figure 1. Scheme of a 3D-micro CT. An X-ray cone beam penetrates the measured object. The object's absorption is recorded by a flat panel detector.

The 3D micro system of the 'Bundesanstalt für Materialforschung und -prüfung' (BAM) used for this study exhibits the following features:

- 30-225 kV microfocus X-ray source with a focal spot size of down to 8  $\mu\text{m}$
- 2048 x 2048 pixel flat panel detector, with CsI-szintillator
- 5 - 200  $\mu\text{m}$  voxel edge length, 110 mm max. object diameter

## 2.2 CT simulation software features

The virtual CT measurements in this study were realized by the aRTist software package [5] of the BAM, developed for computer simulation of industrial radiology applications. The program simulates the whole image forming process. Main elements of the simulation tool are an analytical model for the X-ray penetration process, and the realistic representation of parts under examination.

The X-ray projection process, and thus its model, can be subdivided into three independent parts: the X-ray generation, the interaction between radiation and penetrated material, and the imaging process.

The X-ray source model considers the energy spectrum of the beam and its focal extent. Energy spectra can be calculated by defining X-ray tube parameters, as acceleration voltage and target material, with help of a bremsstrahlung model. But measured spectra or monochromatic radiation for source description are possible as well. A raster of point sources defines the focal spot in its size and radiation density distribution.

The radiation-material interaction with its stochastic processes of absorption and scattering (and pair production for higher energies) can be described by the Boltzmann transport equation. A detailed solution (e.g. using Monte Carlo methods) for arbitrary object geometry is a complex and computing time intensive task and thus not suitable in this case. Therefore, another approach is used here. The ray tracing model applied [6] is based on the attenuation law. The influence of scattered photons and internal sources is considered by the build-up factor or analytical scattering models for single cases.

The imaging process is simulated by tracing beams from all source points to every point in the detector plane. The detector model includes response functions e.g. for the dose to gray value transformation of digital detectors. The inner blurring of the detector is simulated by Gaussian filtering. Noise is added to the synthetic image in consideration of its gray value dependency.

Object geometries under examination are defined by triangulated surface representations. Several geometries can be arranged by Boolean operators within a virtual testing scene. Inside of a boundary surface homogeneous material is considered. Discontinuities can be introduced within the virtual scene by superposition of separated parts of different material. Arbitrary object geometries can be read in using industry standard STL file format. The STL file format describes a triangulated surface by surface normals and vertices using a three-dimensional Cartesian coordinate system. It is also possible to create standard CAD regular geometries (e.g. spheres or cylinders) within the software. Sources of realistic object descriptions may be CAD data, or measurement data from e.g. laser scanners, structured light digitizers or, even CT.

The program comes with a graphical user interface of three basic windows. One presents all parameter settings to control simulation tasks. Another window shows the 3D rendering of the virtual testing scene. An image viewer completes the interface by showing the synthetic exposures. Figure 2 depicts a simulation scenario in the program interface. This example illustrates the inspection of a cast part. The representation of the part consists of more than one million triangles. Also shown in Figure 2 is the synthetic radiography of this part. This image has been calculated assuming a prefiltered 120 kV X-ray spectra and a flat panel detector of 2048 x 2048 pixels. The calculation time was about 40 sec on a standard 3.2 GHz-PentiumIV-PC. While this example shows somewhat the potential of the program the setups in this study were less complex and the computation time for a single projection averages a few seconds only.

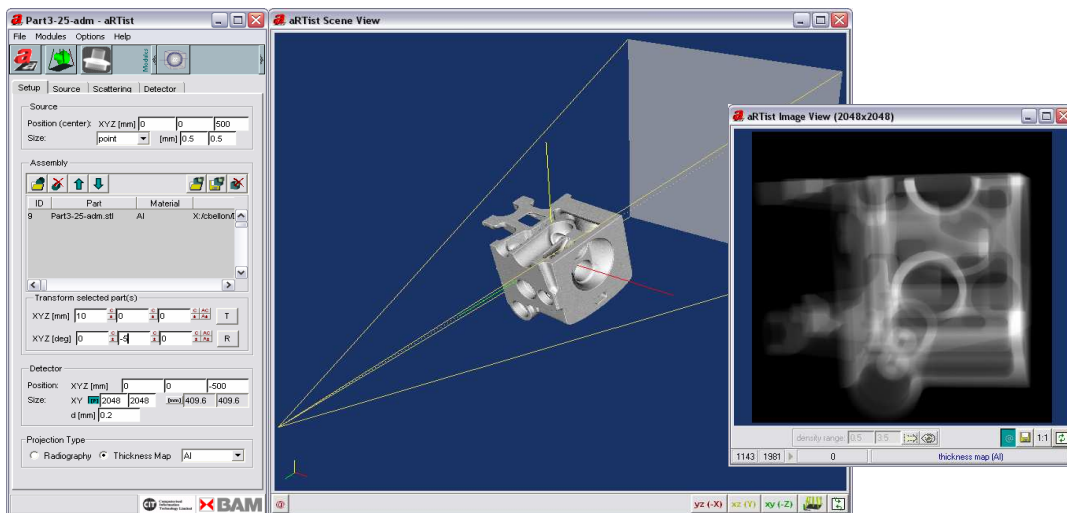


Figure 2. User interface of simulation program “aRTist”.

To support CT investigations an add-on for the aRTist simulation tool was developed. This module automates the scanning procedure of repeating exposures with interim part rotation. Also it collects and saves the projection data in the data format used with the CT systems of the BAM. This enables us to treat the synthetic data exactly like the measured projections of the 3D micro system used for this study.

### **3. Reference standard for CT-measurement and reference data as simulation input**

Important quantities which influence the performance of CT are the relative distances between the source, the object to be measured and the detector, as well as geometrical errors of the mechanical axes. In addition, the size and the shape of the X-ray focus, the X-ray spectrum and the energy-dependent absorption of the object have an influence. The dimension, the geometry and the material composition of the object comprising surface or interface properties such as roughness are influences specific to the object under study. Further influence quantities are the lateral resolution of the detector, the detector properties (energy-dependent sensitivity, signal-to-noise ratio and dynamics) and the preprocessing of the detector signal. Last but not least, there are the tomographic data reconstruction and the reconstructed voxel data postprocessing. Hence, the user's attention must be directed to the careful accomplishing of the CT measurement.

For dimensional measurements, surface point generation has to be carried out as an edge detection process by specifying a threshold value inside the voxel data. Hereafter, the output data form a triangulated surface (polygon data) which can be fed into CAD analysis software. Due to the large number of influence quantities, CT systems often show significant errors which need to be corrected. Certain improvement strategies can be identified:

- Improvement of dedicated components of the CT systems, e.g. X-ray tube with smaller foci, X-ray detectors featuring a higher dynamic range or a better signal-to-noise ratio.
- Improvement of the CT hardware stability by applying techniques from coordinate measuring machines, e.g. by using stable granite base structures, air bearings, linear drives, precision rotary tables, etc.
- Improvement of the CT reconstruction software, e.g. by compensating the energy dependence of absorption and the effects of scattered radiation or by applying reconstruction algorithms which are less sensitive to certain image artefacts (algebraic reconstruction).
- Reduction of systematic measurement errors by the use of calibrated reference standards.

It turned out that the use of calibrated reference standards is the only approach which can be influenced by the CT user himself. It shall therefore be discussed in more detail. The PTB developed reference standards [7] and procedures specifically for applications in the field of CT (see the example in Figure 3).

#### ***3.1 Design, manufacture and calibration of the reference standard***

The reference standards and procedures for CT are currently under development to map guidelines from the field of coordinate metrology to the field of CT. Hence, in this publication, the definitions of dimensional measurement performance characteristics of CT are based on the concepts of classical coordinate metrology i.e. in analogy to the German VDI/VDE 2617-6.2 guideline for optical CMMs. Characteristic parameters such as probing errors and length measurement errors (errors of indication) provide

information on local and global measurement properties of the CT system, respectively. The assessment of these characteristics for CT is carried out by the use of calibrated reference standards similar to those used in coordinate metrology. A high-potential reference standard is the ball plate featuring spherical calottes. The PTB has transferred this concept from coordinate metrology to CT. Ball plates with hemispherically shaped calottes, so-called calotte plates, are suitable for determining several characteristic parameters at the same time. They can be used to check the sphere distance error, the error in sphere diameter and the probing error, and to correct specific measurement errors. The concept of calotte plates is suitable for being scaled down in size and is expandable to 3D [8]. Such a reference standard for micro-CT application has been realised lately in the form of a glass-ceramics plate (Zerodur<sup>®</sup>, Schott AG, Germany) with dimensions of (20 x 20 x 4.5) mm<sup>3</sup> (Figure 3).

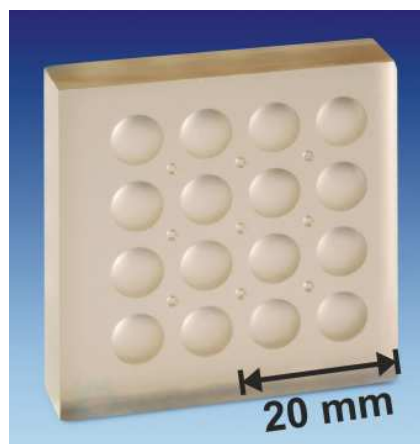


Figure 3. Picture of the reference standard made of Zerodur<sup>®</sup>. A 4 x 4 sphere calotte array was grinded into the plate and polished.

This material is mechanically stable and can be machined precisely. The absolute value of the coefficient of linear thermal expansion is below  $0.5 \cdot 10^{-6} \text{ K}^{-1}$ . Furthermore the material exhibits appropriate X-ray absorption properties for micro-CT applications. The plate, manufactured by PTB by means of multi-level grinding and polishing, features a regular 4 x 4 array of hemispherical calottes having a nominal diameter of 3.0 mm each. The reference standard is calibrated using a reversal method with a tactile coordinate measuring machine (CMM). The single point probing error of the tactile CMM for this measurement task was determined with calibrated convex and concave reference standards having features similar to those on the calotte plate.

By use of the tactile probing points, the centre positions, the diameters and the form deviations of the calottes are calculated. The calibration uncertainties  $U(k=2)$  of the centre positions, the diameters and the form deviations are determined to be 1.5  $\mu\text{m}$ , 2.0  $\mu\text{m}$  and 2.0  $\mu\text{m}$ , respectively.

Using the 3D pointcloud of the probing points the properties of the deduced features are calculated. The deviation of the calottes from the spherical form is less than 2.5  $\mu\text{m}$  for the 10 best calottes, while the maximum form deviation of all calottes amounts to 9.5  $\mu\text{m}$ .

With CT, the problem arises, that the 3D voxel data structure allows symmetry transforms, such as mirrors or parity inversion operations, which can not be expressed by rotations. As a result, there is an uncertainty of obtaining mirrored data instead of

real data. This problem sometimes occurs when comparing different CT systems with different software packages. It is often negligible, though noticeable, for complex measurement objects, but can be important for highly symmetrical objects, as in the case of the sphere calotte plate. Therefore, and because of the more practical reason of having not only regular geometries as measurement task, a sculptured surface segment was merged into the data, that was used for simulation input. The source of the sculptured surface segment was a measurement using optical fringe projection.

A scheme of the process used for generating the reference CAD model utilising the multi-sensor tactile and optical data is shown in Figure 4.

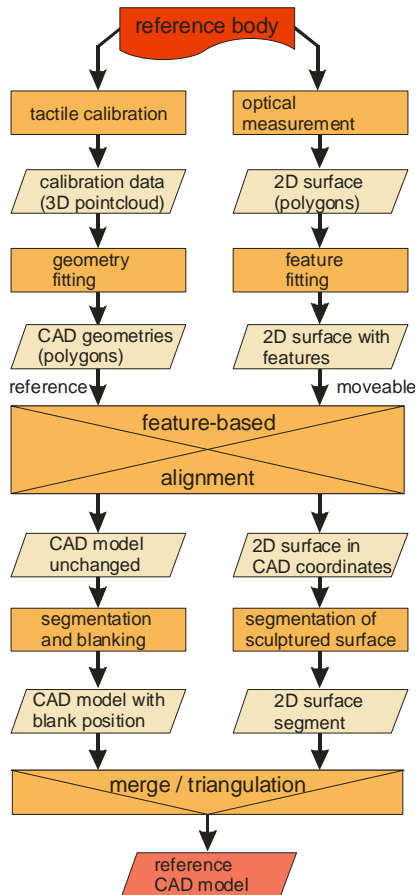


Figure 4. Schematic diagram of the process used to generate the reference CAD model. The square boxes indicate the process steps. The rhombus-shaped boxes indicate a data set as the result of a process step, which may be saved on hard disk as an intermediary result.

engineered CAD dataset (i.e. being the fixed reference here). This alignment is necessary, as the merging of segments from the optical into the reversed engineered CAD dataset will fail otherwise.

After this feature-based alignment, the region of interest (here the sculptured surface) is segmented. The segment is blanked out in the reference model and copied from the optical measurement instead. A final triangulation step merges the segment in a watertight manner into the reference model.

The reference standard is calibrated by means of tactile CMM, which is depicted in Figure 4 on the left process path. In the resulting pointcloud, regular geometries, i.e. spherical calottes and planes representing the object's surface, are fitted using a least-squares-algorithm. As a result, CAD geometries are determined, which can be stored on hard disk as polygonal surfaces. In fact, this process is a reverse-engineering of the calotte plate's surface from the 3D pointcloud.

On the right-hand side of the schematic diagram in Figure 4, the reference standard is measured using fringe projection. The step-by-step process sequence slightly differs from the one on the left-hand side, as the data structure is already a polygonal surface. Therefore the features are only re-fitted for the purpose of gaining information about the features and not for the reverse-engineering of the surface.

Both datasets are now feature-aligned, using the same planes as target features as have been used to form the coordinate system of the workpiece (reference standard) by the tactile measurement. As a result, the optical measurement is transformed into the coordinate system of the reversed

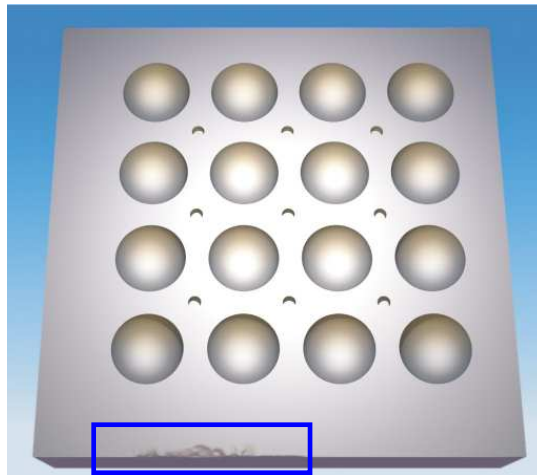


Figure 5. Rendered view of the reference CAD model used as simulation input data. A sculptured surface area was modelled into the dataset as symmetry breaking (see the edge breakage, in the blue frame, bottom left).

Figure 5 shows the completed reference model featuring regions which are close to CAD regular geometries (spheres and planes) and a sculptures surface area. In the triangulation process of the surface a profile shape deviation of  $1.0\ \mu\text{m}$  from the regular geometries was chosen.

### 3.2 Uncertainty of the simulation input data

#### – Determination of manufacturing deviation of the reference standard

In Figure 6, an actual-nominal comparison of the tactile calibration pointcloud (used as actual data in the comparison) with the reverse-engineered reference CAD model (nominal data), is shown.

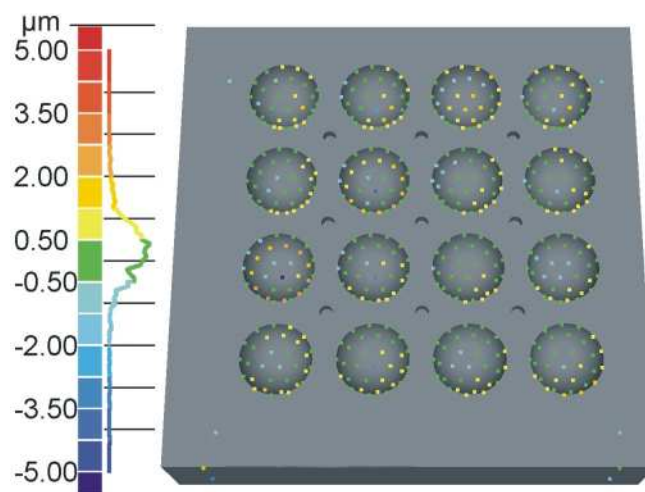


Figure 6. Actual-nominal comparison of the tactile calibration pointcloud and the reference CAD model. Only small form deviations are determined.

The colour-coded deviation between the calibration pointcloud and the reference CAD model displays mainly the form deviation from the regular geometries. From the

histogram shown next to the colour bar in Figure 6, it is observed that 95 % of all deviations are smaller than 1.6  $\mu\text{m}$ .

Taking the calibration uncertainty into account, the obtained residual errors of the reference CAD model are in good agreement with the form deviation of the features of the real standard made of Zerodur given in section 3.1.

As a result of the small deviations it can be concluded, first of all, that the form deviation of the reference standard from the regular geometries due to the manufacturing process is very low. Secondly, the reference model (see Figure 5) renders the reality quite well, except for the residual deviations inherent to the reference standard. It must be noted that the obtained result holds only in the proximity of the tactile probing points.

#### 4. Comparing the measurement with simulation results

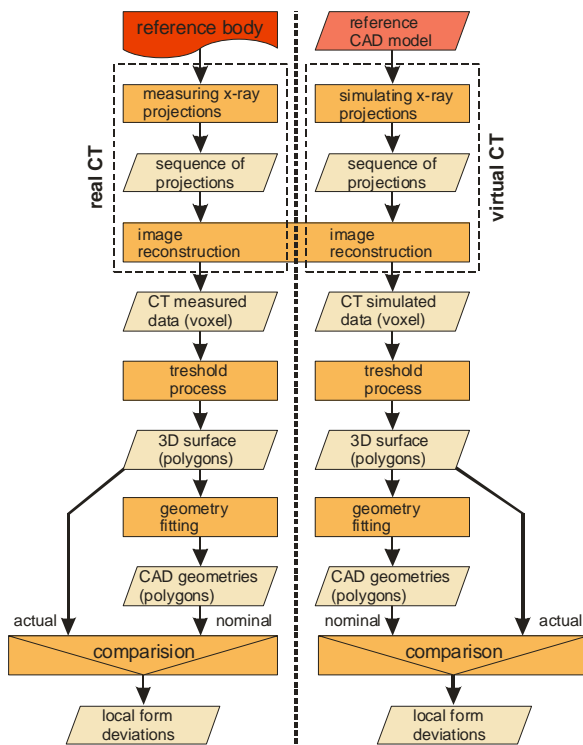


Figure 7. Scheme of CT measurement (left), simulation (right) and evaluation process in analogy to existing guidelines (VDI/VDE 2617-6.2) of coordinate metrology.

In Figure 7, another scheme is shown to visualise the evaluation process of the measurement and the simulation. On the left side of the dashed central line, the workflow of performing and evaluating the real CT measurement is depicted. On the right-hand side the mirrored workflow depicts the process of the virtual CT measurement and its evaluation. With the real CT, the reference standard is measured by recording a sequence of X-ray projections as function of the angle of rotation. The geometry is regained by feeding the projections into the image reconstruction algorithm. The resulting voxel data is post-processed, using a threshold process to separate the material from the background (air) and forming a 3D surface. Subsequently, regular geometries (i.e. spheres) are fitted into the calotte features. The nominal actual comparison of the measured calottes and the fitted calottes yields the local form deviation of the features.

In principle, the process shown on the right is the same. But two details should be pointed out. First of all, instead of the reference standard, the reference model is used as an input. The physical measurement of the reference standard is modelled by the simulation software. Secondly the identical image reconstruction algorithm was used to obtain, in turn, the geometry. Using the identical image reconstruction algorithm is insofar remarkable as it will influence the measurement and the simulation equally and produce equal dimensional deviations.

According to the introduced process chain, the obtained results of the measurement and the simulation are presented in section 4.2. The examination is performed in analogy to the German guideline VDI/VDE 2617-6.2.

Applying this guideline allows to separate the measurement properties of CT into dimensional measurement characteristics, like sphere center distances and sphere diameters on the one hand and form measurement characteristics on the other hand. The according characteristics are designated as sphere distance error, error of diameter and probing error, respectively.

It is noteworthy that the guideline can be used to judge both the measurement result of the real CT and the simulated result of the virtual CT.

#### 4.1 Characteristic parameters of the CT measurement

Adopting the use of ball plates for CMMs, the calotte plate can be measured in different orientations in the measurement volume, to determine the spatial distribution of errors. Hence, two micro 3D-CT measurements were carried out with the same parameters to validate the procedure. The acceleration voltage has been chosen to be 150 kV (with 0,03 mm copper and 0,025 mm tin as preliminary filter) and the resulting voxel edge length was about 30  $\mu\text{m}$ .

In Figure 8, the result of the calotte centre position error of the first measurement is shown. In this measurement, the calottes were arranged horizontally in the middle of the measurement volume. In the sketch, the difference vectors between the calibrated centre positions (arrow head) and the CT-measured positions (arrow base) are plotted. The CT system of the BAM features a relative deviation of sphere distances of about 0.5% (lengths are measured too short).

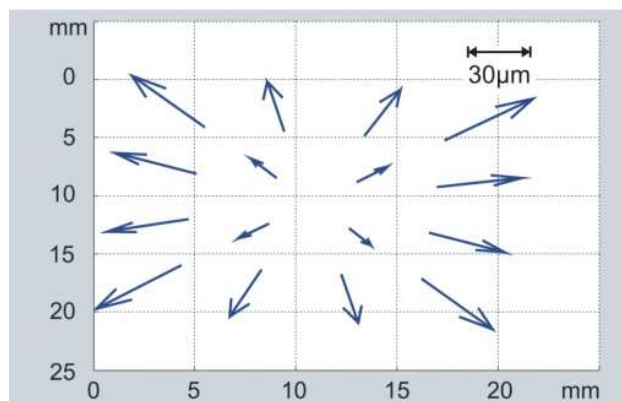


Figure 8. Calotte centre position errors (state before performing scale error correction) of a micro CT measurement performed with the Zerodur calotte plate at 150 kV acceleration voltage and  $(30 \mu\text{m})^3$  voxel size. The arrows representing the position errors are magnified. The relative length scale is given in the upper right corner.

In a second measurement, the calotte plate was turned vertically so that it was positioned parallel to the axis of rotation of the CT system. The same scale error was observed. After correcting the scale errors, the residual errors were analysed and are sketched in Figure 9 in analogy to DIN EN ISO 10360 Part 2. A maximum residual error of  $\pm 6.5 \mu\text{m}$  can be observed.

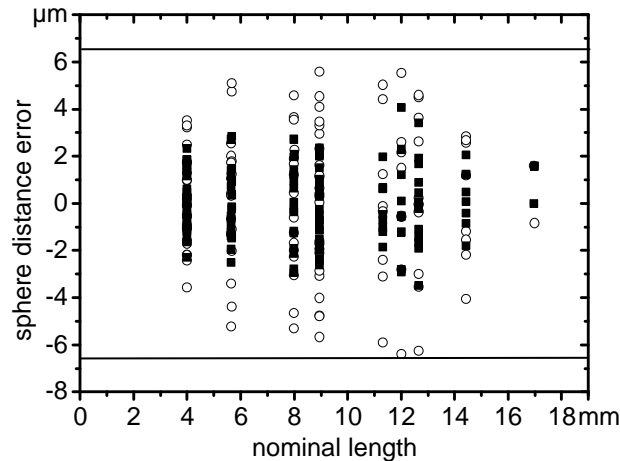


Figure 9. Residual calotte distance errors after correction of scale error. The solid squares indicate results with horizontal arrangement, the open circles indicate results with vertical arrangement of the reference standard.

Due to the fact that the sphere distance error is systematic in the geometrical assembly of the CT system, and was reproduced by repeated measurement, it can be automatically corrected within the reconstruction process of the object geometry. By applying a scale correction, sphere distance errors smaller than half the voxel edge length are achieved. It was found that the spread of the vertical measurement was larger than that of the horizontal measurement. This behaviour has been reproduced by several different CT systems and is of a systematic nature. It must be noted that the spread of the horizontal measurement is in the range of the calibration uncertainty of the reference standard, which is the limit for the correction.

After correction of the scale error and determination of the sphere distance errors, the error of size of the calotte diameter was evaluated. In Figure 10 the error of diameter is given as number next to each calotte. The obtained result that the errors of diameter are not evenly distributed around zero indicates, that the threshold is not optimally adjusted and that there is further potential for minimising the errors. Finally the calotte plate allows assessment of the probing errors (radial span of measured calotte surface relative to local least squares sphere fit) which can be evaluated locally for each calotte. In this way, one can analyse the spatially anisotropic behaviour of the CT system. Furthermore, the magnitude of the local form deviation can be displayed as colour coded spatial distribution (Figure 10). A clear dependence of the errors on the measurement orientation of the calotte plate can be identified by the distribution of the colour coded form deviation.

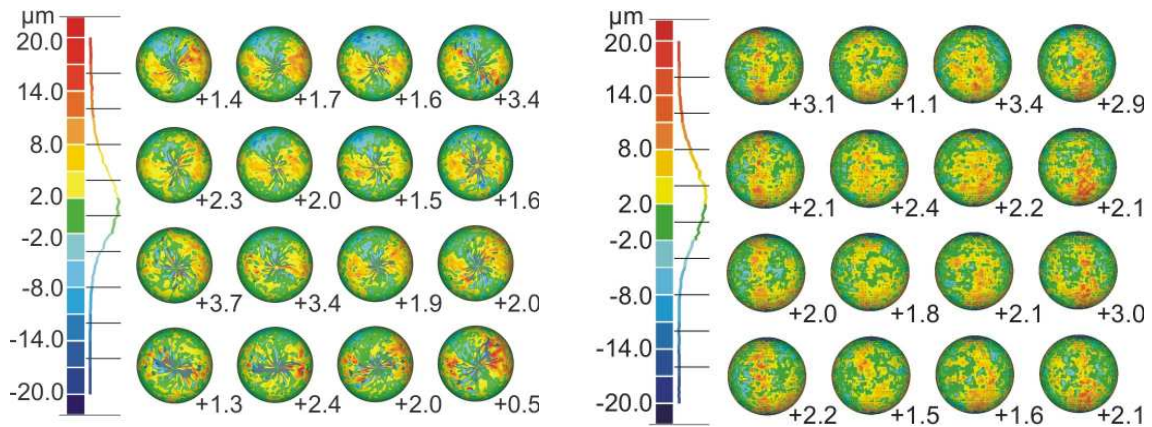


Figure 10. Colour coded form deviation of calotte surface obtained by measurement, relative to local least squares sphere fit [9]. The calottes are viewed as coloured spheres from the inside of the reference standard. The histograms indicate the overall distribution of the form deviation. The numbers next to each calotte indicate the error of diameter of the local fitted spheres to the calibrated diameter in units  $\mu\text{m}$ :  
 Left-hand side: Measurement result in horizontal orientation;  
 Right-hand side: Measurement result in vertical orientation of the reference standard in the measurement volume of the real CT.

The CT measurement induces form deviations of  $\pm 15 \mu\text{m}$  (about the voxel edge length of  $30 \mu\text{m}$ ) which are significantly larger than the real form deviation ( $2.5 \mu\text{m}$ ) of most of the calottes.

Major CT measurement errors producing the observed symmetry dependent form deviation were supposed to be ring artefacts or beamhardening effects from the variable penetrated material thickness. The systematic nature of the observed form deviations on the orientation of the calotte plate was proofed by repeating the measurements with different CT systems, too.

The demonstrated method is thus a new and powerful tool for the CT developer to analyse, quantify and correct different measurement errors. The results presented were gained using the micro CT system of the BAM. Other results, obtained with other micro CT systems suggest, that measurement errors scale with the voxel size also after correction. Hence, smaller measurement errors can be expected with new detectors having even more pixels.

#### ***4.2 Characteristic parameters of the CT simulation***

As shown before, the dimensional measurement characteristics of CT can be improved considerably by the use of a calibrated reference standard, however the form measurement still suffers from uncorrected errors.

To characterize the influence quantities to the form measurement characteristics, the measurement was simulated using the aRTist simulation software.

The simulation of the X-ray projections was performed as close to reality as possible concerning our current understanding of the underlying measurement.

The source was modelled as point-source, with a simulated spectrum of 150 kV acceleration voltage and tungsten target, taking also the absorption of the preliminary filters into account.

The flat panel detector was modelled with 0.4 mm lateral resolution, with a transfer function for dose to gray value, a noise by dose, two weighted convolution filters to taking into account the blurring caused by internal carrier diffusion and internal

scattering. A white image correction was applied to each simulated projection modelling the gain and offset of the detector pixel. It was found, that ring artefacts appeared in the reconstructed voxel data, if noise was added to the white image correction.

All parameter needed for simulation were taken either directly from the measurement or, from the measured X-ray projections, i.e. the exposure time, the intensity level, and the signal to noise ratio.

In Figure 11, the result of the evaluation process sketched in Figure 7 is shown. It can be immediately observed, that the distribution of the colour coded form deviation differs for both positions of the reference standard in the virtual measurement volume of the CT as in the case of the real CT. That the spatial distribution of the local form deviation is reproduced is seen best for the vertical orientation on the right hand side of Figure 11. The histograms indicating the overall distribution of the deviations are in quantitative agreement with the measured ones (compare Figure 10).

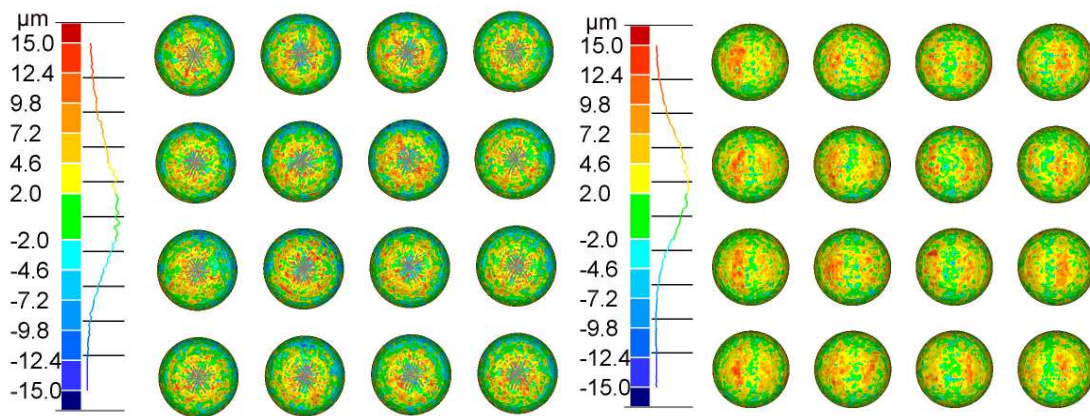


Figure 11. Colour coded form deviation of calotte surface obtained by simulation, relative to local least squares sphere fit. The simulations were performed with ‘best simulation capability’ to match the measurement, with simulated 150 kV spectra and preliminary filter, noise and ring artefacts. The results are displayed for the different orientation of the reference CAD model in the measurement volume of the virtual CT. Left-hand side: Horizontal orientation; Right-hand side: Vertical orientation.

Several simulations were performed and evaluated by a systematic variation of parameters from their maximum value obtained from the measurement to a vanishing value at zero. Last but not least, two simulations were performed without any noise, nether in the single projection, nor in the white image correction (which means no ring artefacts in the reconstructed voxel data). Beamhardening effects were disabled using monochromatic radiation for calculation (at 70 keV beam energy). The results of the evaluation are depicted in Figure 12.

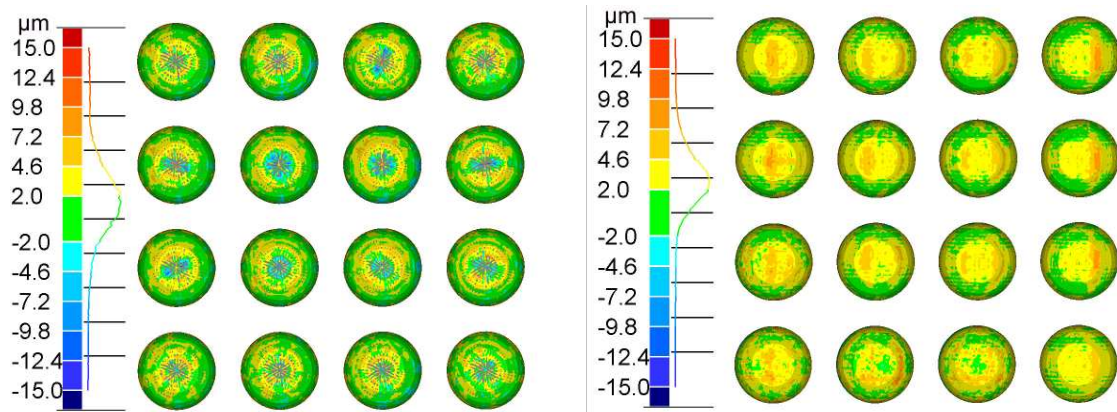


Figure 12. Colour coded form deviation of calotte surface obtained by simulation, relative to local least squares sphere fit. The ideal simulations were performed with monochromatic radiation, no noise and without ring artefacts. Left-hand side: Horizontal orientation; Right-hand side: Vertical orientation.

Although all effects which obviously lead to systematic and statistic form deviations are switched of in the two simulation results, the characteristic form deviations of the calottes still remain visible. It can be seen from the histogram next to the colour tables in Figure 12, that the width of the distribution is much lower as in the case with added noise, ring artefacts, and beamhardening (compare Figure 11). This is a clear evidence, that the magnitude of the form deviation is weaker, now about in the sub voxel range.

Only the simulations without negative effects on the form deviation give, for the first time, a clear hint where the systematic form deviation originates. Two parameters have not taken into account yet. At first it may be supposed the observed symmetry dependent form deviations are an artefact of the sampling of the reference standard, or the reference CAD model, respectively. In particular the number of projections of about 900 has not been changed during measurement and simulation.

Another influence factor on the form deviation may be the reconstruction algorithm itself. As the identical image reconstruction algorithm is used to calculate the object geometry for both, the measurement and the simulation it may be possible that the reconstruction produces the symmetry dependent form deviation.

Further studies will be drawn out separate and quantify these influence factors on the measurement properties of the CT, too.

## 5. Conclusion

Industrial CT exhibits an ongoing development. Many dimensional measurement tasks can already be performed with the present CT systems. In addition, CT is the only nondestructive measurement technique which is able to perform also measurements of inner geometries. The method of correcting CT data by using reference standards, which has been presented here, can significantly improve the accuracy of dimensional measurements. Up to now, these techniques have been applied to the correction of scale errors and the assessment of threshold values. First results indicate that with corrected CT, dimensional measurement characteristics, like sphere distance error, and the error of diameter are achievable that are in the range far below the voxel edge length.

As in coordinate metrology, reference standards can be used to determine more complex characteristic parameters. Procedures and guidelines are under development. The

definition of characteristics is currently under discussion in the German standardisation bodies (VDI/VDE-GMA Technical Committee 3.33).

The analysis of the magnitude of the influence quantities is a challenge for such a complex technique as CT. It could be shown that simulation is an advantageous tool to aid this process. The influence of noise, ring artefacts and beamhardening on the form measurement characteristics of CT measurement could be revealed for the first time. The presence of these influences significantly impair the form measurement properties of CT measurements to the range of about the voxel edge length.

A process was introduced applying existing guidelines of coordinate metrology to the field of CT. With this process meaningful characteristics can be deduced to obtain detailed information of the measurement characteristics. The process was also successfully used to compare CT measurement with simulation results.

### **Acknowledgments**

The first part of the presented work, particularly the CT measurements, was supported by the 'Bundesministerium für Wirtschaft und Technologie' (BMW) with the project number VI A 2-08/03. Current activities are supported by the Deutsche Forschungsgemeinschaft (DFG) with the project number NE 757/2-1.

The authors wish to thank Mr. Albert Dettmer and Mr. Konrad Hierse, both PTB, for the manufacturing and calibration of the Zerodur calotte plate.

### **References**

1. J Hsieh 'Computed tomography: principles, design, artifacts, and recent advances', SPIE Press monograph, PM114, 2003.
2. GUM: ISO/BIPM-Guide 'Guide to the Expression of Uncertainty in Measurement', 1995.
3. H-C Saewert, D Fiedler, M Bartscher and F Wäldele 'Obtaining dimensional information by industrial CT-scanning – present and prospective process chain', DGZfP Conference book BB 84-CD, 2003.
4. B P Flannery, W G Roberge and K A D'Amico 'Three-Dimensional X-Ray Microtomography', Science, Vol 237, 1987.
5. C Bellon, G-R Jaenisch 'aRTist - analytical Radiographic Testing inspection simulation tool', proceedings of DIR2007, Lyon, 2007.
6. C Bellon 'Computersimulation radiographischer Prüfverfahren', PhD thesis, Dresden University of Technology, Logos-Verlag, Berlin, 2001.
7. M Bartscher, D Fiedler, H-C Saewert and F Wäldele 'Dimensionelle Messabweichungen eines industriellen 2D-Computertomographen: Einfluss der Werkstückgeometrie', VDI-Bericht 1829, 2004.
8. M Neugebauer, U Hilpert, M Bartscher, N Gerwien, S Kunz, F Neumann, J Goebels, G Weidemann 'Ein geometrisches Normal zur Prüfung von Röntgen-Mikrocomputertomographiemesssystemen' submitted to: Technisches Messen, Oldenbourg-Verlag, München.
9. M Bartscher, U Hilpert, J Goebels, G Weidemann 'Enhancement and Proof of Accuracy of Industrial Computed Tomography Measurements', Annals of the CIRP Vol. 56/1/2007.